International Conference on Applied Energy 2019
Aug 12-15, 2019, Västerås, Sweden
Paper ID: xxxx

INVESTIGATION ON THE SPRAY DEVELOPMENT PROCESS OF GASOLINE-BIODIESEL BLENDED FUEL SPRAYS IN A CONSTANT VOLUME CHAMBER

Kihyun Kim [1], Shubhra Kanti Das[2], Dinh Nam Vu[2], Jaeheun Kim[3], Ock Teack Lim [2*]
[1]Division of Mechanical Convergence Engineering, Silla University
[2]School of Mechanical Engineering, University of Ulsan
[3]Graduate School of Engineering, Hiroshima University
Corresponding Author: Ock Teack Lim, E-mail address: otlim@ulsan.ac.kr

ABSTRACT

This study investigates a fuel spray development process of gasoline–biodiesel blended fuel (GB) in macroscopic and microscopic scales. Long-distance microscopy and shadowgraph were utilized as optical methods to capture the highly transient spray development. Different injection pressures were tested, which ranged from 40 to 120 MPa with a fuel temperature of 323K. Tested four fuels were neat gasoline and biodiesel addition (5%, 20%, 40% by volume) to gasoline in three different ratios. The results regarding the development process for the initial spray near the nozzle show that the spray penetration and the spray tip velocity both decreased with decreasing biodiesel blending ratio. This relationship appears to be due to the associated differences in the mass flow rate and the radial direction velocity vector of the spray. In addition, the different spray tip velocities at the start of spraying result in different atomization regimes between the fuels. The GB fuels with the low biodiesel blending ratio were disadvantaged in spray atomization due to their lower spray penetration and tip velocity. However, as the injection pressure increased, the differences in microscopic spray penetrations between the fuels became smaller, along and there were changes in the atomization characteristics.

Keywords: gasoline, biodiesel, sprays, shadowgraph, long distance microscopy, atomization

1. INTRODUCTION

Compression ignition (CI) engines are fuel-efficient engines which due to their high compression ratio and lack of throttling losses. Recently, advanced combustion strategies with lean mixtures and low-temperature combustion have been studied to reduce harmful emissions, such as NOx (nitric oxides) and PM (particulate matter) emissions, while maintaining high levels of thermal efficiency. The proposed combustion strategies are homogeneous charge compression ignition (HCCI) and premixed charge compression ignition (PCCI). These combustion strategies normally adopt moderately early injection timing to achieve an active mixing process between fuel and air, so that lean combustion can be implemented [1].

Gasoline-like fuels have higher volatility and lower ignitability compared to diesel-like fuels and so are called low reactivity fuels. Gasoline-like fuels that perform with high ignition delays leading to longer mixing time due to the low reactivity have recently been tested in advanced combustion strategies to improve the mixing of fuel and air. It was reported that gasoline-like fuels are advantageous in achieving mid to high load conditions with significantly low fuel consumption and emissions, but with high emissions of HC and CO and combustion instability under low load conditions. These problems under low loads are due to the excessively high resistance to autoignition of gasoline fuels, and thus, many researchers have found that fuels with octane numbers of about 70–80, which are lower than for conventional high-octane fuels, are more suitable than high-octane fuels for gasoline CI engines. Therefore, a number of researchers have tested dieseline, which is a mixture of diesel and gasoline, in CI engines. Zhang et al. [12] used dieseline to conduct a direct injection study. Although fuel blends may add complexity, they provide researchers a design and control tool for fuel properties. The direct mixing of gasoline and diesel before injection can avoid stratification in the cylinder, along with the benefit of minimal modification to current injection systems; however, researchers need to thoroughly study their combined chemical and physical properties [2].

Biodiesel's lower volatility compared to diesel fuel promotes its longer liquid spray penetration. Due to biodiesel's high oxygen content, complete combustion

Selection and peer-review under responsibility of the scientific committee of the 11th Int. Conf. on Applied Energy (ICAE2019).

is possible. Adams studied the effect of biodiesel–gasoline blends on gasoline compression ignition (GCI) combustion by examining 5 and 10% biodiesel using a partially premixed, split-injection strategy, finding that these additions of biodiesel significantly reduced the intake temperature requirement. They also concluded that higher NOx and lower CO and UHC were emitted, due to gasoline's higher averaged spatial bulk temperature. Yanuandri compared GB20 (gasoline 80%, biodiesel 20%) and diesel fuel modes in a single-cylinder diesel engine to investigate peak pressure rise rate, combustion phasing, ignition delay, and NOx and HC emissions. They observed a shorter ignition delay and less HC emission using GB20.

The current study was performed to investigate the spray development processes for neat (100%) gasoline and for gasoline blended with biodiesel through microscopic and macroscopic visualizations. The spray development process is determined by both the physical properties of the fuel and the injection parameters. The physical properties vary with the blending ratio, enabling us to investigate their effects on the spray development process. We varied the fuel injection pressure to examine the effect of spray velocity on the spray development process. We conducted both micro- and macroscopic visualization techniques to discover the sequential or causal relationships of the spray development from the nozzle tip to downstream of the spray.

2. EXPERIMENTAL SETUP AND CONDITIONS

2.1 Fuel properties

Table 1 Physical properties of the GB00, GB05, GB20, and GB40 fuels used in this study

Property	Unit	Test method	GB00	GB05	GB20	GB40	B100
Density at 15 °C	kg/m^3	KS M ISO 12185:2003	712.7	722.3	757.1	789.3	882.3
Lubricity	mm	KS R ISO 12156-1:2012	548	290	236	212	189
Cloud point at 15 °C	15°C	KS M ISO 3015:2008	-57	-57	-16	-8	3
Kinematic viscosity at 40 °C	mm^2/s	KS M ISO 3104:2008	0.735	0.9097	1.4338	2.1326	4.229
Heating value	MJ/kg	ASTM D240:2009	45.86		43.6	43.6	39.79
Surface tension at 20 °C	mN/m	ASTM D971:2009	18.93	19.56	21.53	24.07	31.7
Stoichiometric air–fuel ratio	-		14.7		14.276	13.852	12.58
Octane number (RON)	-		91		-	-	-
Cetane number (CN)	-		16.38		23.9	31.43	54
Blend ratio of gasoline	-		1.0	0.95	0.80	0.60	-

2.2 Experimental setup and optical arrangenments

Table 2. Experimental conditions and optical setup for spray visualization

Ambient conditions		
Ambient gas density (kg/m^3)		1.2
Ambient temperature (K)		310
Fuels		GB00, GB05, GB20, GB40
Fuel temperature (K)		313
Injector type		Bosch Solenoid CRIN 2
Nozzle orifice diameter (mm)		0.30
Injector nozzle type		Single hole SAC
Injection pressure (MPa)		40, 80, 120
Injection duration (μs)		1000
Optical setup	**Microscopic imaging**	**Macroscopic imaging**
Light source		Solid state laser MGL-W-532nm
Frame rate (frame/sec)	8000	40000
Exposure time (us)	0.37	3.25
Image resolution (pixel*pixel)	1024*752	512*256
Scaling factor (mm/pixel)	0.004	0.179
Aperture	f/2.8	f/2.8

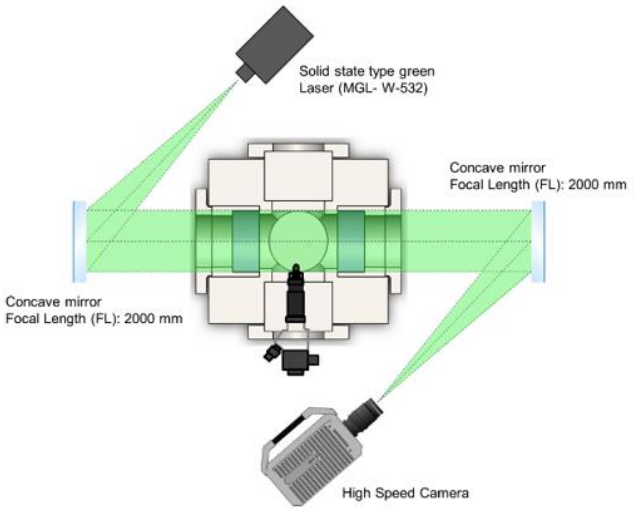

Fig 1. Optical setups for macroscopic and microscopic spray visualization.

2.3 Spray analysis method

We acquired the spray penetration, spray angle, projected area, particle sizes, and total numbers of particles through image post-processing. We used the spray projected area for microscopic images as an alternative indicator to the spray angle. We did this because the spray in the vicinity of the nozzle interacts with ambient air vigorously, and the value of the spray angle is greatly dependent on the selection of distance downstream from the nozzle tip. It is difficult to capture an accurate spray angle by simply drawing a triangle of a certain height over the spray because the periphery of the side of the spray cannot be interpreted as a simple straight line. In addition, the spray is highly asymmetric across the spray axis near the nozzle. Therefore, the spray area provides more intuitive results of how much the spray has dispersed radially. For macroscopic images, the conventional spray angle was calculated to indicate spray dispersion. We acquired the spray penetration, spray angle, projected area, particle sizes, and total numbers of particles through image post-processing. We used the spray projected area for microscopic images as an alternative indicator to the spray angle. We did this because the spray in the vicinity of the nozzle interacts with ambient air vigorously, and the value of the spray angle is greatly dependent on the selection of distance downstream from the nozzle tip. It is difficult to capture an accurate spray angle by simply drawing a triangle of a certain height over the spray because the periphery of the side of the spray cannot be interpreted as a simple straight line. In addition, the spray is highly asymmetric across the spray axis near the nozzle. Therefore, the spray area provides more intuitive results of how much the spray has dispersed radially. For macroscopic images, the conventional spray angle was calculated to indicate spray dispersion.

3. RESULTS AND DISCUSSION

3.1 Microscopic spray characteristics

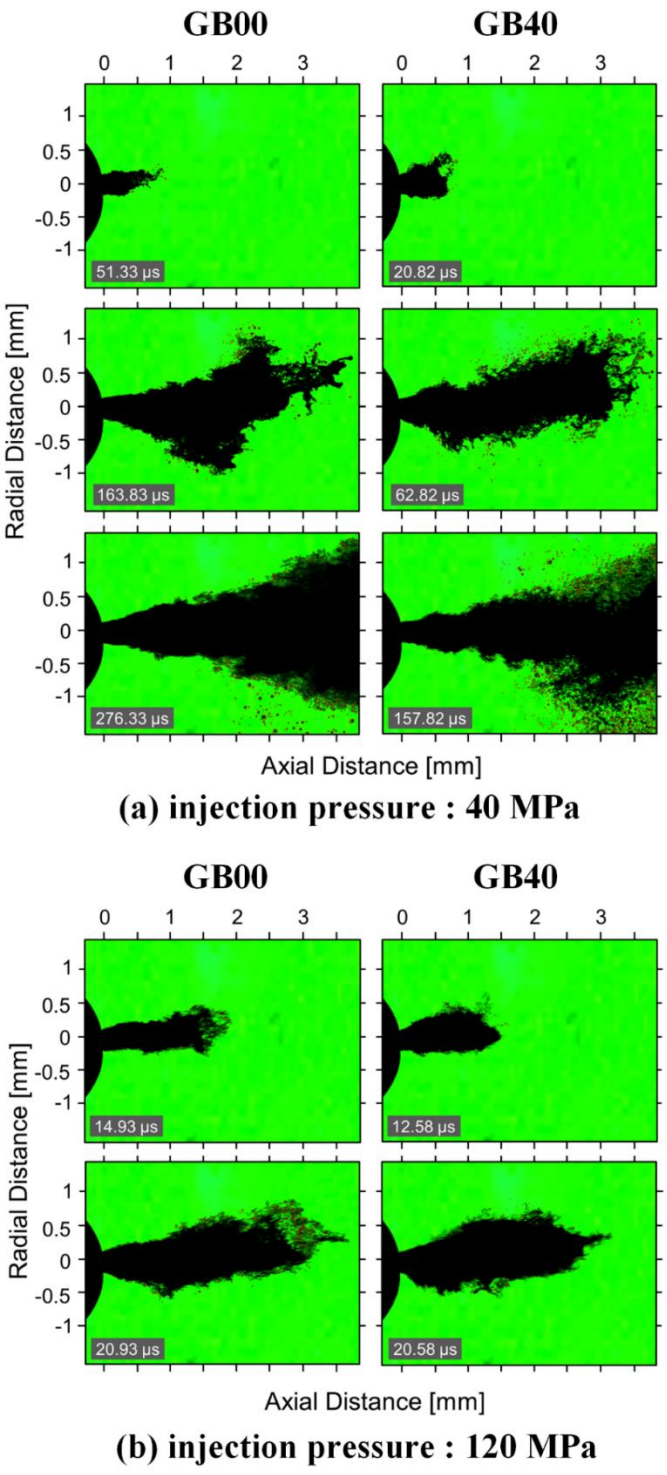

Fig 2. Microscopic images under injection pressures of (a) 40 MPa, and (b) 120 Mpa.

Fig 2 shows an example of the initial spray development process at injection pressures of 40 and 120 MPa for GB00 and GB40 fuel in the vicinity of the nozzle tip. The start of injection (SOI) timing (0 ms ASOI) is defined as the time of first appearance of the fuel from the nozzle in the microscopic images, but not the start of the energizing time by the injection signal pulse. Therefore, any injection delay caused by the different fuel types or injection pressure can be neglected. It can be seen from the second row of images in Fig 2(a) that the GB40 fuel took a shorter time to achieve the same penetration as that of the GB00 fuel under the injection pressure of 40 MPa, which also means there was a higher spray tip velocity for the GB40 fuel. However, the difference in penetration between the two fuels almost disappeared under the injection pressure of 120 MPa (Fig 2(b)).

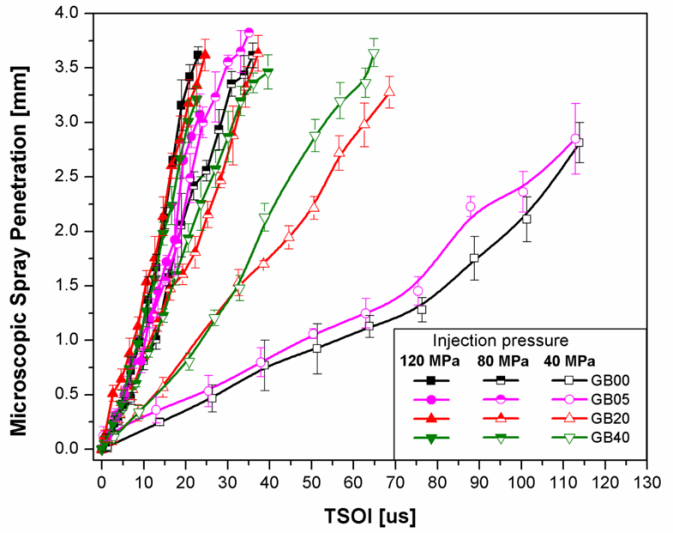

Fig 3. Microscopic spray penetration of GB fuels according to the injection pressure.

Fig 3 shows the microscopic spray penetration under different injection pressures and fuel types. Similar to the results shown in Fig 2, the spray penetration was shorter for GB fuels with lower biodiesel blending ratios and the low injection pressure of 40 MPa. The spray penetrations for the GB00 and the GB05 fuels were similar, and those for the GB20 and the GB40 fuels exhibited similar penetrations. Overall, the spray penetration increased as the blending ratio of the biodiesel increased. Moreover, the difference in spray penetrations of the different fuels was remarkably reduced as the injection pressure increased. This is consistent with observations of the raw images shown in Fig 2.

3.2 Macroscopic spray characteristics

Fig 4 shows the spray penetrations of all tested fuels over time after start of injection. The average values over six injection events are presented. The spray evolution of all tested fuels under atmospheric pressure revealed a narrow spray structure due to less interaction with the ambient gas and little effects by aerodynamic forces due to the high-density ratio of the liquid and gas. This results from both the high injection

rate and the high viscous fuel characteristics. A higher viscous fuel causes difficulty in the dispersion and the breakup process in air entrained spray boundary, but potentially increases axially, which is a reason for the increasing tip penetration. The macroscopic spray penetration of biodiesel fuel is usually higher compared to gasoline fuel, which has been reported experimentally and numerically in various studies. However, an increase in injection pressure attenuates these fuel-specific property effects on penetration, which leads to less deviation among GB00, GB05, GB20, and GB40 in temporal spray development. However, we still observed a slightly higher macroscopic spray penetration for GB40 than for GB00. Microscopic spray penetration showed little difference according to the blending ratio of fuel. However, as the spray developed, the spray penetration of the fuels with higher blending ratios of biodiesel increased faster due to the fuel properties, especially the high viscous characteristic. Therefore, we conclude that the spray penetrations of the fuels with higher ratios of biodiesel were slightly greater due to the fuel properties, even under increased injection pressure.

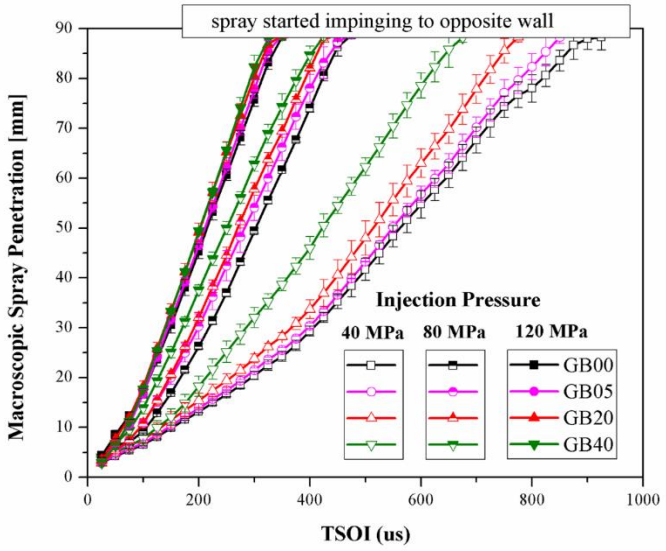

Fig 4. Macroscopic spray penetration of GB fuels according to the injection pressure.

4. CONCLUSIONS

Results of the microscopic spray visualization showed that the GB fuels with lower biodiesel blending ratios under low injection pressure showed lower spray tip velocity compared to the rest of the fuels. The lower velocity yielded disadvantages in the initial spray atomization process. We observed fewer ligaments and droplets during spray development of GB fuels having lower biodiesel blending ratio.

The GB fuels with lower biodiesel blending ratios had wider spray cone angles in the macroscopic spray visualization because the low viscosity and the surface tension characteristics increased the shearing instability in the vicinity of the spray. However, because of the spray's highly transient nature and the asymmetric shape at the beginning of spray development, microscopic spray visualization was unable to clearly show the radial diffusion characteristics through observation of the spray cone angle or spray projected area. Therefore, to predict the macroscopic spray diffusion rate in the radial direction, more elaborate microscopic analysis are required, such as regarding the amount of spray asymmetry, variability of spray axis, and shape of spray.

Microscopic spray visualization and macroscopic spray visualization showed similar trends for spray penetration distance. Through the macroscopic spray visualization, we observed that the spray penetration length was shorter for GB fuels with lower biodiesel blending ratios. The difference decreased as the injection pressure was increased, but the tendency was maintained. We judged the shorter spray penetration length to be caused by the active dispersion in the spray radial direction due to lower viscosity and surface tension characteristics. Therefore, It is concluded that a GB fuel with a high gasoline blending ratio interacts more actively between the spray and ambient air.

In this study, we determined a correlation between microscopic spray analysis and macroscopic spray analysis. To analyze the spray atomization process over its entire duration, it is necessary to expand the range of microscopic spray analysis and to perform much more elaborate analysis. We plan to carry out further research based on this conclusion.

ACKNOWLEDGEMENT

This research was financially supported by the CEFV (Center for Environmentally Friendly Vehicle) as Global-Top Project of KMOE (2016002070009, Development of Engine System and Adapting Vehicle for Model 110cc and 300cc Correspond to EUERO-5 Emission), and by The Leading Human Resource Training Program of Regional Neo industry through the National Research Foundation of Korea (NRF) funded by The Ministry of Science, ICT and Future Planning (2016H1D5A1908826).

REFERENCE

[1] G. Najafi, B. Ghobadian, T. Tavakoli, D.R. Buttsworth, T.F. Yusaf, M. Faizollahnejad, Performance and exhaust emissions of a gasoline engine with ethanol blended gasoline fuels using artificial neural network, Appl. Energy 86 (2009) 630-639.

[2] Mahdizadeh Khasraghi M, Gholami Sefidkouhi MA, Valipour M. Simulation of open- and closed-end border